Journal of Alloys and Compounds 480 (2009) 806–809

Contents lists available at ScienceDirect

Journal of Alloys and Compounds

journal homepage: www.elsevier.com/locate/jallcom

Influence of temperature on thermophysical properties of EB-PVD porous coatings and dense ceramics of 4 mol% Y_2O_3-stabilized ZrO_2

Byung-Koog Jang*

Nano Ceramics Center, National Institute for Materials Science, 1-2-1 Sengen, Tsukuba, Ibaraki 305-0047, Japan

ARTICLE INFO

Article history:
Received 6 November 2008
Received in revised form 4 February 2009
Accepted 13 February 2009
Available online 4 March 2009

Keywords:
Electron beam physical vapor deposition
Y_2O_3-stabilized zirconia
Thermal diffusivity
Thermal conductivity
Nanopore

ABSTRACT

This work describes the experimental results of thermal diffusivities, thermal conductivities, and thermal resistivities of single coatings, double coatings, and sintered ceramics of 4 mol% Y_2O_3-stabilized ZrO_2 in a temperature range from room temperature to 1000 °C. The fractured surface of the coated samples revealed a columnar microstructure. The thermal conductivities and thermal diffusivities of both EB-PVD coatings and sintered ceramics decreased with increasing temperature. The thermal diffusivities and thermal conductivities of double-layer coatings were lower than those of single-layer coatings and sintered ceramics at a given temperature.

1. Introduction

Thermal barrier coatings (TBCs) are widely used in gas turbine engines to protect the underlying metal from the high operating temperature and improve the durability of the components and engine efficiency [1–4]. TBCs generally consist of 7–8 wt% yttria-stabilized zirconia (YSZ) with a high thermal expansion coefficient and low thermal conductivity and chemical inertness in combustion atmosphere [5–8].

The YSZ top coats for TBCs were applied by either electron beam physical vapor deposition (EB-PVD) [9] or air plasma spray (APS) [10]. EB-PVD TBCs are used on advanced turbine blades to increase engine efficiency and improve blade performance at high operating temperatures because of their favorable properties, such as their strain-tolerant columnar microstructure, good thermal shock resistance, strong bonding to the substrate, and smooth surface of the coatings [11–13].

Thermophysical properties including thermal conductivity is one of the most important properties in the design of TBCs for high temperature application of gas turbine blades since the thermal efficiency by temperature drops across the coatings can be controlled by the thermal conductivity and operating temperature. Some investigations have already been reported regarding the relationship between the thermal conductivity and the microstructure of TBCs [14–20].

However, the influence of the temperature and microstructure of single-layer coatings and multi-layer coatings on thermophysical properties at the same YSZ composition has not been thoroughly investigated. For this reason, the present work is focused on this point.

The aim of this study is to determine the influence of the temperature on thermophysical properties, such as thermal diffusivity, thermal conductivity, and thermal resistivity of EB-PVD YSZ porous coatings as well as of a sintered dense YSZ sample for comparison. For this purpose, single-layer coatings and double-layers coatings were deposited by EB-PVD.

2. Experimental procedure

4 mol% Y_2O_3-stabilized ZrO_2 coatings by EB-PVD were applied to disc-shaped YSZ substrates of 10.0 mm diameter. For the comparison of the thermophysical properties, sintered dense YSZ specimens of 10 mm diameter and 1.0 mm thickness were prepared by pressure sintering at 1500 °C for 2 h. The coating process was carried out using EB-PVD equipment (Von Ardenne Anlagentechnik).

A coating chamber under 1 Pa vacuum was used with a commercially available 63 mm diameter YSZ ingot (Daiichi Kigenso Co.) and a 45-kW electron beam gun. The substrate temperature was 950 °C.

The average coating thickness for single-layer coatings was about 300 μm at stationary substrate. Later coatings with 150 μm for double-layer coatings were consecutively conducted on the top surface of previous coatings layer with 150 μm which cool down to room temperature.

The deposition rate for double-layer coatings was about 5 μm/min at 1 rpm of substrate rotation speed. The porosity of the samples was obtained by taking the difference between the density of the coated samples (as determined by measuring their mass and volume) and the theoretical density (6.05 g/cm^3) of ZrO_2–4 mol%Y_2O_3. Free standing EB-PVD coatings were obtained by machining the substrate from the coated specimen prior to thermal conductivity measurements.

* Tel.: +81 29 859 2453; fax: +81 29 859 2401.
E-mail address: JANG.Byungkoog@nims.go.jp.

0925-8388/$ – see front matter © 2009 Elsevier B.V. All rights reserved.
doi:10.1016/j.jallcom.2009.02.091

The thermal diffusivity of the specimens was measured in a vacuum chamber with a temperature range of 25–1000 °C at 200 °C intervals with a laser flash technique [21] using a thermal analyzer (Kyoto Densi, LFA-501). Because of the translucency of the specimens to the laser, the specimens were sputter-coated with a thin layer of silver and colloidal graphite spraying to ensure complete and uniform absorption of the laser pulse prior to the thermal diffusivity measurement. The laser flash method involves heating one side of the sample with a laser pulse of short duration and measuring the temperature rise on the rear surface with an infrared detector. The thermal diffusivity is determined from the time required to reach one-half of the peak temperature in the resulting temperature rise curve for the rear surface.

The specific heat of the specimens was also measured in the same temperature range during heating using a differential scanning calorimeter (Netzsch, DSC 404C) with reference materials of single-crystal alumina under argon gas. The experimental thermal conductivity of the specimens was then obtained according to the following relationship:

$$k = \alpha \cdot C \cdot \rho \quad (1)$$

where k is the thermal conductivity, α is the thermal diffusivity, C is the specific heat, and ρ is the density of the specimens. The microstructure of the coated samples was observed by SEM.

3. Results and discussion

3.1. Microstructure of EB-PVD coatings

A typical micrograph of single-layer and double-layer coatings of ZrO_2–4 mol%Y_2O_3 obtained by EB-PVD is shown in Fig. 1. The fracture surfaces of these layer coatings clearly reveal a textured microstructure with all the columnar grains oriented in the same direction, i.e., with the c axes perpendicular to the substrate. The widths of the columnar grains vary according to the distance from the substrate despite the columns having the same crystallographic orientation [22]. In addition, it was reported that the preferred crystallographic growth directions of columns in the coatings are ⟨1 0 0⟩ [23].

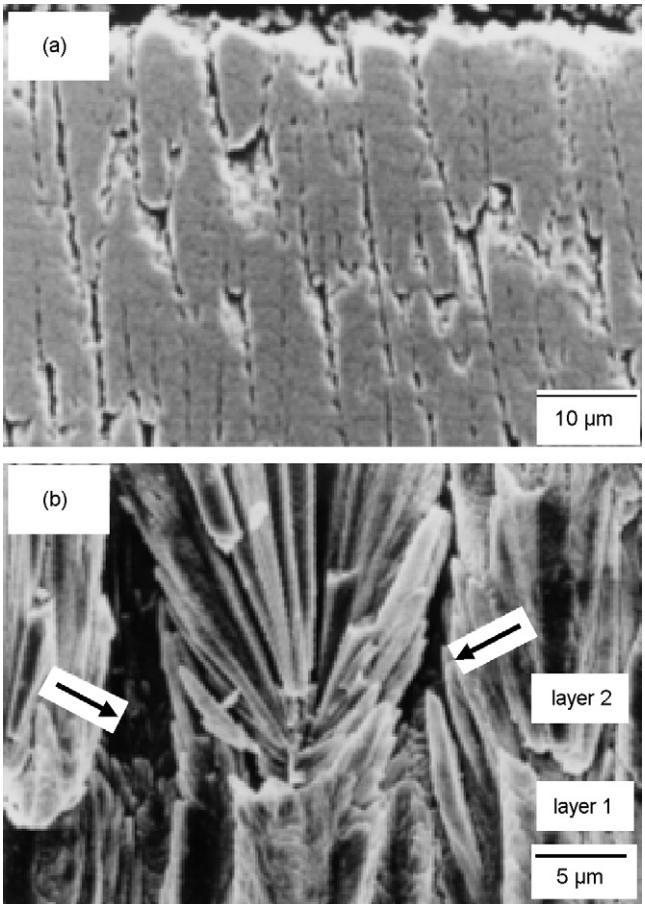

Fig. 1. SEM micrographs of 4 mol%Y_2O_3–ZrO_2 coatings obtained by EB-PVD: (a) single-layer coatings and (b) interface at double-layer coatings (the arrows show the layer-interface pores).

Table 1
Porosity of EB-PVD coatings and sintered ceramics of 4 mol%Y_2O_3–ZrO_2.

Samples	Porosity (%)
Double-layer coatings	22.4
Single-layer coatings	9.1
Sintered body	0.5

The main difference between single and double layers in the present sample coatings was in the porosity and interface properties. In other words, more pores can be easily formed at the interface of inter-layers during double-layer than single-layer deposition. When a subsequent layer is deposited on the top surface of the previous layer for double-layer coatings, some space at inter-layers can exist due to the roughness of the top surface of the columns of the previous layer [23], which results in the formation of pores as well as a non-uniform interface.

Table 1 shows the porosity of EB-PVD coatings and sintered ceramics of ZrO_2–4 mol%Y_2O_3. The porosity of the coated sample is higher than that of the sintered sample. This means that the columnar structure of coatings has many pores, such as intercolumnar gaps, intragranular nanopores within columns, and nanopores at feather-like features of the columns [22]. In addition, the porosity of double-layer coatings is higher than that of single-layer coatings due to the formation of pores at the interface. This microstructural result can have an effect on the thermophysical properties, which are discussed in the next chapter.

3.2. Thermophysical properties

Fig. 2 shows the representative temperature-rise response behavior as a function of time on the rear surface of specimens after laser pulse heating for sample double-layer coatings. The time which reaches the maximum temperature in the temperature rise curve increased with an increase in the measuring temperature. This tendency is the same for single-layer coatings and sintered samples.

To determine the thermal diffusivity, the following temperature response on the rear surface of the specimen is obtained [21]:

$$\Delta T = \Delta T_m \left[1 + 2\sum_{i=1}^{\infty}(-1)^n \exp\left(\frac{-n^2\pi^2}{L^2}\alpha t\right)\right] \quad (2)$$

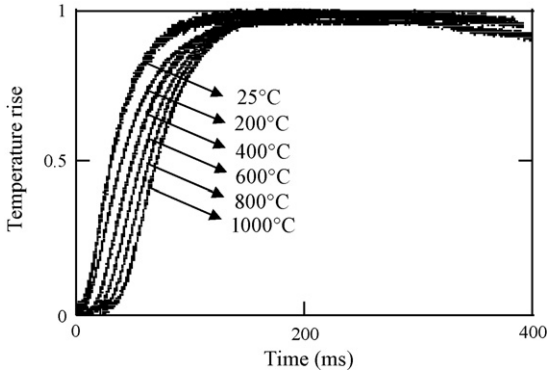

Fig. 2. Temperature rise curve as a function of time on the rear surface of specimens after laser pulse heating at high temperature for double-layer coatings obtained by EB-PVD.

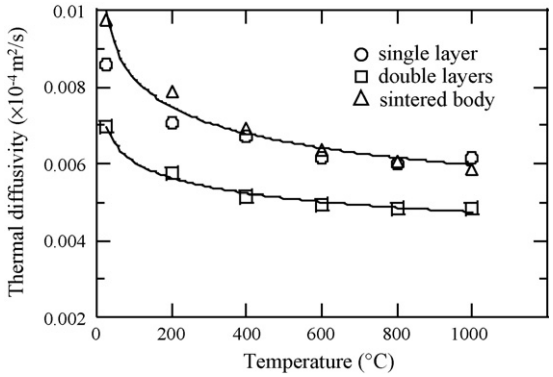

Fig. 3. Thermal diffusivity vs. temperature of EB-PVD coatings and sintered ceramics of 4 mol%Y_2O_3–ZrO_2.

where α and L are the thermal diffusivity and the thickness of the specimen, respectively, ΔT is the temperature rise of the specimen, ΔT_m is its maximum value, and t is the time after pulse heating.

The thermal diffusivity (α) is described by the following equation:

$$\alpha = \frac{1.38L^2}{\pi^2 t_{1/2}} \tag{3}$$

where L is the thickness of the specimen and $t_{1/2}$ is the time period corresponding to a temperature rise to half of the maximum temperature on the rear surface of the specimens.

Fig. 3 shows the thermal diffusivities of the present specimens as a function of the measurement temperature. The figure shows that the thermal diffusivities of the coated specimens decrease with the increase in temperature. The present results are in agreement with that of thermal diffusivities for single-layer coatings with higher porosity in the previous report [24].

The thermal diffusivities of double-layer coatings are significantly lower than those of a single-layer coating or sintered body at a given temperature. This is caused by the high porosity and non-uniform interface of double-layer coatings, which results in the enhancement of phonon scattering.

The thermal conductivities of specimens are plotted as a function of the temperature in Fig. 4. The thermal conductivities of the sintered specimens show a distinct tendency to decrease with increasing temperature. The thermal conductivities of EB-PVD coatings decrease slightly with increasing temperature. It was reported that thermal conductivity of partially yttria-stabilized zirconia (P-YSZ) EB-PVD coatings decreased with increasing temperature [14].

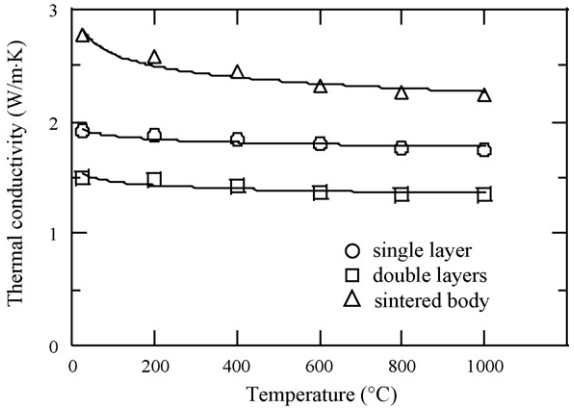

Fig. 4. Thermal conductivity vs. temperature of EB-PVD coatings and sintered ceramics of 4 mol%Y_2O_3–ZrO_2.

In addition, it is apparent that the thermal conductivities of the coatings are remarkably lower than those of the sintered samples. Based on this result, the porous columnar microstructure in the coatings can be considered to be the dominant factor for obtaining lower thermal conductivity. In particular, the reason that the thermal conductivity of double-layer coatings is lower than that of single-layer coatings is a microstructural difference, such as high porosity and a non-uniform interface with micro-pores, as shown in Fig. 1. In addition, it was reported that the thermal conductivity on room temperature for multi-layer coated specimens decreases with increasing number of coating layer [25–27]. Wolfe et al. fabricated multi-layer coatings with about 120–133 μm between 1 and 20 layers [27]. In their report [27], the grain size was found to decrease with the increasing number of layers for the TBCs, resulting in lower thermal conductivity.

The influence of pores on lower thermal conductivity can be explained as follows. This is consistent with results showing that the porosity and/or defects provide a major contribution to the reduction of the thermal conductivity of plasma-sprayed coatings [28,29]. Furthermore, the porous interfacial microstructure in double-layer coatings is very similar to those reported for the splat microstructure (lamellar and cracked microstructure) coated by plasma-sprayed coatings [28,29]. It has been reported that the splat boundaries in plasma-sprayed coatings lead to the greatest decrease in thermal conductivity [29].

In general, the presence of defects, for example pores, vacancies, grain boundaries and inclusions, has been greatest effect in decreasing the thermal conductivity of a solid. Pores and interface primarily decrease the net section area through which heat can be transported by phonon and so the reduction in thermal conductivity depends not only on the volume fraction but also on the architecture of pores [30]. This can be explained from the theory of thermal conductivity by phonons (lattice waves).

In the fundamental work of the Debye phonon approximation [31–33], the thermal conductivity can be expressed as an integral over temperature T:

$$k = \frac{k_B}{2\pi^2 \nu}\left[\frac{k_B}{h}\right]^3 T^3 \int_0^{\theta/T} \frac{\tau(x)x^4 e^x dx}{(e^x-1)^2} \tag{4}$$

where ν is an appropriately averaged velocity of sound and k_B and h are Boltzmann's and Planck's constants, respectively. θ is the Debye temperature, $x = h\omega/k_B T$, and $\tau^{-\tau}(x)$ is the scattering rate at temperature T for a phonon of frequency ω.

Therefore, the lattice vibration of the thermal conductivity can be written by [31]:

$$k = \frac{1}{3}\int_0^{\omega_{\max}} C(\omega, T)\nu(\omega)l(\omega, T)d\omega \tag{5}$$

where $C(\omega)d\omega$ is the contribution to specific heat of the vibration modes, which have a frequency between ω and $\omega + d\omega$, $\nu(\omega)$ is the phonon velocity, and $l(\omega,T)$ is the phonon mean free path.

The mean free path (l) of a phonon can be expressed as follows:

$$\frac{1}{l} = \frac{1}{l_p} + \frac{1}{l_i} \tag{6}$$

where l_p and l_i are, respectively, the phonon–phonon scattering contribution and the phonon-impurity scattering contribution, such as the interfaces, interstitials, grain boundaries, vacancies, and lattice strain.

As observed from Eqs. (4)–(6), if the phonon mean free path by the increase of phonon scattering at pores or defects can be decreased, it can be understood that thermal conductivity decreases. Consequently, in double-layer coatings, a high porosity with micro- and/or nanopores as well as a non-uniform interface will additionally limit the mean free path of phonons

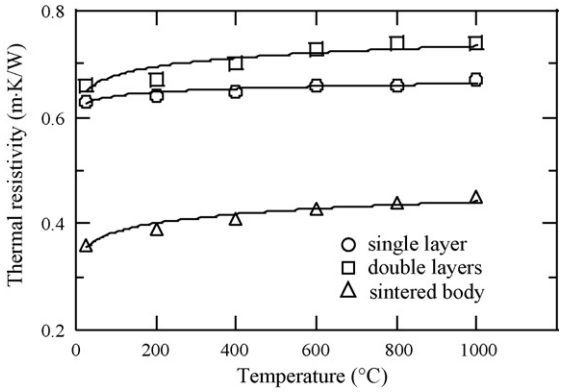

Fig. 5. Thermal resistivity vs. temperature of EB-PVD coatings and sintered ceramics of 4 mol%Y_2O_3–ZrO_2.

and thus contribute to a further decrease in thermal conductivity.

To evaluate the heat transport behavior, the thermal resistivities of the present specimens can be obtained by the reciprocal of the thermal conductivity values. The thermal resistivities of specimens are plotted as a function of the temperature in Fig. 5. Although the thermal resistivities of single-coating specimens reveal a slight increase, their values for the present specimens show an increasing tendency with increasing temperature. Their values of all specimens reveal the almost constant above 800 °C. This means that the heat transport in the present specimens is by lattice thermal conduction being known as phonon contribution. In the lattice mode of heat transport, it is known that the phonon mean free path gradually decreases with increasing temperature, resulting in an increase in the thermal resistivities due to the increase of phonon scattering.

For this case, the explanation on radiative thermal conductivity considering the effect of photon in the transport of heat must be necessary [34,35].

4. Conclusions

The thermophysical properties of EB-PVD porous coatings and sintered dense ceramics of 4 mol% Y_2O_3-stabilized ZrO_2 were investigated in a temperature range of 25–1000 °C. EB-PVD coatings had a porous columnar microstructure with gaps between columnar grains. The thermal conductivities of the EB-PVD coatings were remarkably lower than those of the sintered samples. Their values showed a decreasing tendency with increasing temperature. In addition, the thermal diffusivity and thermal conductivity of double-layer coatings were found to be lower than those of single-layer coatings. This result was attributed to the enhancement of phonon scattering due to the formation of many pores at the interface and the non-uniform interface in double-layer coatings. In addition, the thermal resistivities of the present specimens showed an increasing tendency with increasing temperature.

Acknowledgment

This work was carried out with financial support from the New Energy and Industrial Technology Development Organization (NEDO), Japan.

References

[1] N.P. Padture, M. Gell, E.H. Jordan, Science 296 (2000) 280.
[2] R.A. Miller, J. Therm. Spray Technol. 6 (1999) 35.
[3] D.J. Wortman, B.A. Nagaraj, E.C. Duderstadt, Mater. Sci. Eng. A 120–121 (1989) 433.
[4] D. Zhu, R.A. Miller, MRS Bull. 25 (2000) 43.
[5] R.A. Miller, Surf. Coat. Technol. 30 (1987) 1.
[6] P.K. Wright, Curr. Opin. Solid State Mater. Sci. 4 (1999) 255.
[7] S. Stecura, Am. Ceram. Soc. Bull. 56 (1977) 1082.
[8] T.E. Strangman, Thin Solid Films 127 (1985) 93.
[9] R.A. Miller, J.L. Smialek, R.G. Garlick, in: A.H. Heuer, L.W. Hobbs (Eds.), Advances in Ceramics, vol. 3, Science and Technology of Zirconia, American Ceramic Society, Columbus, OH, 1981, pp. 241–253.
[10] D.D. Hass, P.A. Parrish, H.N.G. Wadley, J. Vac. Sci. Technol. 16 (1998) 3396.
[11] U. Schulz, K. Fritscher, H.J.R. Scheibe, W.A. Kaysser, M. Peters, Mater. Sci. Forum 251–254 (1997) 957.
[12] M. Peters, C. Leyens, U. Schulz, W.A. Kaysser, Adv. Eng. Mater. 4 (2001) 193.
[13] J.R. Nicholls, MRS Bull. 9 (2003) 659.
[14] U. Schulz, H.J.R. Scheibe, B. Saruhan, A.F. Renteria, Mater. Werkstofftech. 38 (2007) 659.
[15] U. Schulz, J. Münzer, U. Kaden, Ceram. Eng. Sci. Proc. 23 (2002) 353.
[16] D. Zhu, R.A. Miller, B.A. Nagaraj, R.W. Bruce, Surf. Coat. Technol. 138 (2001) 1.
[17] A. Azzopardi, R. Méverl, B.S. Ramond, E. Olson, K. Stiller, Surf. Coat. Technol. 177–178 (2001) 131.
[18] J.R. Nicholls, K.J. Lawson, A. Johnstone, D.S. Rickerby, Mater. Sci. Forum 595 (2001) 369.
[19] J. Singh, D.E. Wolfe, J. Singh, J. Mater. Sci. 37 (2002) 3261.
[20] B.K. Jang, H. Matsubara, Scripta Mater. 54 (2006) 1655.
[21] W.J. Parker, R.J. Jenkins, C.P. Butler, G.L. Abbott, J. Appl. Phys. 32 (1961) 1679.
[22] B.K. Jang, H. Matsubara, Surf. Coat. Technol. 200 (2006) 4594.
[23] U. Schulz, S.G. Terry, C.G. Levi, Mater. Sci. Eng. A 360 (2003) 319.
[24] B.K. Jang, H. Matsubara, J. Alloys Compd. 419 (2006) 243.
[25] B.K. Jang, Surf. Coat. Technol. 202 (2008) 1568.
[26] J. Singh, D.E. Wolfe, R.A. Miller, J.I. Eldridge, D.M. Zhu, J. Mater. Sci. 39 (2004) 1975.
[27] D.E. Wolfe, J. Singh, R.A. Miller, J.I. Eldridge, D.M. Zhu, Surf. Coat. Technol. 190 (2005) 132.
[28] R. Dutton, R. Wheeler, K.S. Ravichandran, K. An, J. Therm. Spray Technol. 9 (2000) 204.
[29] J.R. Nicholls, K.J. Lawson, A. Johnstone, D.S. Rickerby, Surf. Coat. Technol. 151–152 (2002) 383.
[30] T.J. Lu, C.G. Levi, H.N.G. Wadley, A.G. Evans, J. Am. Ceram. Soc. 84 (2001) 2937.
[31] P.G. Klemens, in: R.P. Tye (Ed.), Thermal Conductivity, vol. 1, Academic Press, London, UK, 1969, pp. 1–68.
[32] W.D. Kingery, Introduction of Ceramics, John Wiley, New York, 1960.
[33] R. Berman, Thermal Conduction in Solids, Oxford University Press, Oxford, 1976.
[34] G.J. Hyland, J. Nucl. Mater. 113 (1983) 125.
[35] D.R. Clarke, Surf. Coat. Technol. 163–164 (2003) 67.